Optical Trapping and Control of a Dielectric Nanowire by a Nanoaperture

ARTICLE *in* OPTICS LETTERS · SEPTEMBER 2015

Impact Factor: 3.29 · DOI: 10.1364/OL.40.004807 · Source: arXiv

3 AUTHORS:

Mehdi Shafiei Aporvari

University of Isfahan

5 PUBLICATIONS **14** CITATIONS

SEE PROFILE

Fardin Kheirandish

University of Isfahan

61 PUBLICATIONS **250** CITATIONS

SEE PROFILE

Giovanni Volpe

Bilkent University

88 PUBLICATIONS **1,300** CITATIONS

SEE PROFILE

Optical Trapping and Control of a Nanowire by a Nanoaperture

Mehdi Shafiei Aporvari,[1,2,*] Fardin Kheirandish,[1] and Giovanni Volpe[2,3]

[1] *Department of Physics, Faculty of Science, University of Isfahan, Isfahan, Iran.*
[2] *Soft Matter Lab, Department of Physics, Bilkent University, Ankara 06800, Turkey.*
[3] *UNAM – National Nanotechnology Research Center, Bilkent University, Ankara 06800, Turkey*

We demonstrate that a single sub-wavelength nanoaperture in a metallic thin film can be used to achieve dynamic optical trapping and control of a single dielectric nanowire. A nanoaperture can trap a nanowire, control its orientation when illuminated by a linearly-polarized incident field, and also rotate the nanowire when illuminated by a circularly-polarized incident field. Compared to other designs, this approach has the advantages of a low-power driving field entailing low heating and photodamage.

Optical manipulation and control of nanoparticles is potentially important in many areas of physical and life sciences [1]. In particular, controlling the position and orientation of elongated objects leads the way towards exciting applications: in nanotechnology, optically trapped semiconducting nanowires have been translated, rotated, cut and fused in order to realize complex nanostructures [2–4]; in spectroscopy, the composition and morphology of a sample have been probed by scanning optically trapped nanowires [5] and polymer nanofibres [6] over the sample's surface; in biophysics, many bacteria, viruses and macromolecules with rod-like shapes have been optically manipulated and studied [7]. However, optical manipulation of nanoobjects is particularly challenging; in fact, the techniques developed for optical manipulation of microparticles and, in particular, standard three-dimensional optical tweezers — i.e., tightly focused laser beams capable of confining microparticles [8, 9] — cannot be straightforwardly scaled down to the nanoscale. This is mainly due to the fact that optical forces scale down with particle volume and are ultimately overwhelmed by the presence of thermal fluctuations [1]. Recently, several novel approaches have been put forward to overcome such limitations [1, 10–12]. Thanks to the strong field enhancement associated with plasmonic resonances, plasmonic optical traps have been particularly successful in trapping ever smaller particles down to single molecules [11]. Furthermore, by altering the illumination conditions it has been possible to control the properties of the trap, e.g., tuning the strength of a plasmonic trap [10] and rotating an optically trapped particle around a plasmonic nanopillar [12]. Also, hybrid plasmonic fields arising from the interaction between the surface plasmon polaritons (SPPs) along a metal surface and the localized surface plasmons (LSP) on a metallic nanowire have been employed to trap and controllably orient a single gold nanowire [13].

Amongst the various metallic nanostructures that have been employed for plasmonic optical manipulation, subwavelength apertures in thin metal films have generated a considerable amount of interest [14–17]. Extraordinary optical transmission was first observed on arrays of nanoholes in metallic films, where it was due to the coupling of light to SSPs excited in the periodically patterned metal film [18]. Later, it was demonstrated that, even for a single nanohole in a flat metal surface, the excitation of LSPs on the aperture ridge can alter its transmission properties [19]; in particular, the electric field intensity pattern was shown to display two high intensity spots parallel to the polarization direction of the incident light and attributed to a dipole moment oriented in the plane of the metal film and parallel to the axis joining the spots. One of the main advantages of using subwavelength nanoholes for optical trapping is that they permit one to reduce the required local intensity compared with conventional trapping, therefore significantly reducing the likelihood of optical damage [11].

The main idea of the work presented in this Letter is to use the intensity distribution with two hotspots generated at a nanoaperture as a handle to trap and control elongated objects such as nanowires. We show that nanoapertures can be efficiently used to trap dielectric nanowires with low power and to control their orientation and movement through the polarization of the input beam. Compared to previous designs, the approach we propose has the advantages of a low-power driving field and an extremely simple design.

As shown in Fig. 1a, we consider a dielectric nanowire with radius r and length L placed at a distance h above a cylindrical nanoaperture of radius 155 nm in a 100-nm-thick gold film. A linearly-polarized plane wave with wavelength 1064 nm illuminates the sample from the side opposite to the one where the nanowire lies. The long axis of the nanowire lies on the xy-plane at an angle θ with respect to the polarization direction. The medium is water (refractive index $n_\mathrm{m} = 1.33$). We compute the electromagnetic field with a three-dimensional finite-difference time-domain (3D-FDTD) algorithm together with a total-field/scatter-field technique and employing a small grid size (less than 3 nm) in order to account for all plasmonic near-field behaviors [20]. We bound the simulation domain with a convolutional perfectly matched layer (CPML) [20]. For the dielectric constant of the film, we use the Drude model with parameters that fit

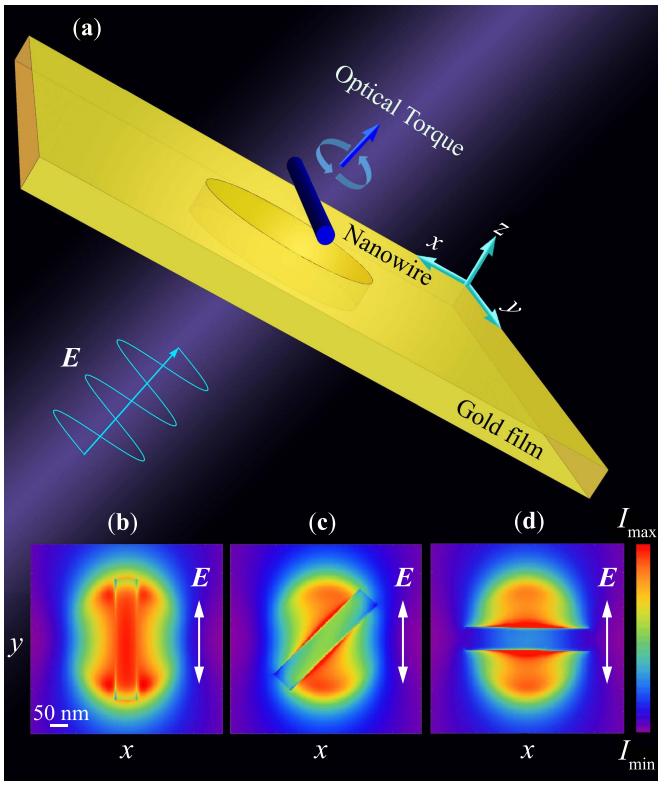

FIG. 1. (color online) (**a**) Schematic of the configuration for the optical trapping and control of a nanowire by a nanoaperture. (**b**)-(**d**) Electric field intensity distribution in the xy-plane passing though the center of the nanowire (length $L = 350\,\text{nm}$, radius $r = 30\,\text{nm}$, medium refractive index $n_\text{m} = 1.33$) for various orientations of the nanowire, i.e., (**b**) $\theta = 0$, (**c**) $\theta = \pi/4$ and (**d**) $\theta = \pi/2$. The nanowire is placed 50 nm above the nanoaperture. The incident electric field is a plane wave linearly-polarized along the direction indicated by the arrows in (**b**)-(**d**) with input intensity $I_0 = 1.0\,\text{mW}\mu\text{m}^{-2}$.

the experimental values of the dielectric data for gold [21]. Figs. 1b-d show the intensity distributions in the xy-plane passing through the center of a nanowire placed at a distance $h = 20\,\text{nm}$ above the metal film with various orientations. There are two hotspots on the rim of the nanohole along the incident field polarization direction. As we will see in the following, the nanowire tends to align itself along the direction of these hotspots and, thus, this effect can be exploited to control the nanowire's orientation.

Once the electromagnetic fields have been calculated using 3D-FDTD, we proceed to calculate the optical forces and torques acting on the nanowire using the Maxwell stress tensor (MST) method [22]. The time-averaged force and torque acting on the center of mass of the nanowire are

$$\langle \mathbf{F} \rangle = \int_S \langle \mathbb{T} \rangle \cdot \hat{\mathbf{n}}\, dS \tag{1}$$

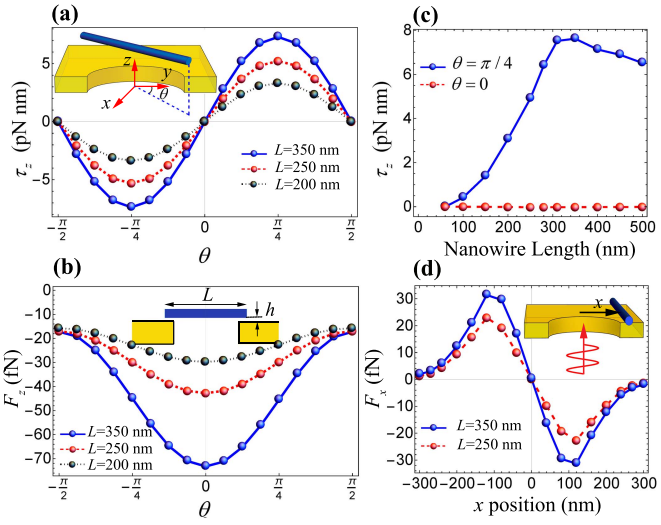

FIG. 2. (color online) (**a**) Optical torque, τ_z, and (**b**) normal optical force, F_z, on a nanowire of length $L = 200$, 250 and 300 nm trapped above a nanohole as a function of the angle θ between the nanowire and the incident filed polarization (along the y-direction). (**c**) Optical torque on a nanowire as a function of its length L with $\theta = \pi/2$ and 0. (**d**) The lateral optical restoring force, F_x, acting on nanowires of length $L = 250$ and 350 nm. In all cases, $r = 30\,\text{nm}$, $h = 20\,\text{nm}$ and $I_0 = 1.0\,\text{mW}\mu\text{m}^{-2}$.

and

$$\langle \boldsymbol{\tau} \rangle = -\int_S \langle \mathbb{T} \rangle \times \mathbf{r} \cdot \hat{\mathbf{n}}\, dS\,, \tag{2}$$

where S is a surface enclosing the nanowire, $\hat{\mathbf{n}}$ is the unit vector perpendicular to the surface, $\mathbf{r}$ is the position of the surface element, and $\langle \mathbb{T} \rangle$ is the time-averaged Maxwell stress tensor for harmonic fields, i.e.,

$$\langle \mathbb{T} \rangle = \frac{1}{2}\Re\left\{\epsilon \mathbf{E}\,\mathbf{E}^* + \mu \mathbf{H}\,\mathbf{H}^* - \frac{\mathbf{I}}{2}\left(\epsilon|\mathbf{E}|^2 + \mu|\mathbf{H}|^2\right)\right\}\,, \tag{3}$$

where $\mathbf{E}$ is the electric field, $\mathbf{H}$ is the magnetic field, and ϵ and μ are the permittivity and permeability of the surrounding medium.

Fig. 2a shows the torque acting on the nanowire along the z-axis as a function of its orientation θ with respect to the incident field polarization direction. The torque magnitude is maximum at $\theta = \pm\pi/4$ and zero at $\theta = 0$ (stable equilibrium) and $\pm\pi/2$ (unstable equilibrium). Therefore, the nanowire tends to align itself with the polarization of the incident electromagnetic field. The origin of this orientation is in the induced dipole moment on a non-spherical particle. In fact, since the external electric field induces a dipole moment $\mathbf{p} = \boldsymbol{\alpha} \cdot \mathbf{E}$, where $\boldsymbol{\alpha}$ is the polarizability tensor, the electrostatic torque exerted on the particle is $\boldsymbol{\tau} = \frac{1}{2}\Re\{\boldsymbol{p} \times \mathbf{E}^*\}$. Considering a symmetric ellipsoid, this torque is $\tau_z = \alpha_\text{eff} E^2 \sin(2\theta)$, where $E = |\boldsymbol{E}|$, $\alpha_\text{eff} = \Re\{\alpha_\text{long} - \alpha_\text{trans}\}$, α_long and

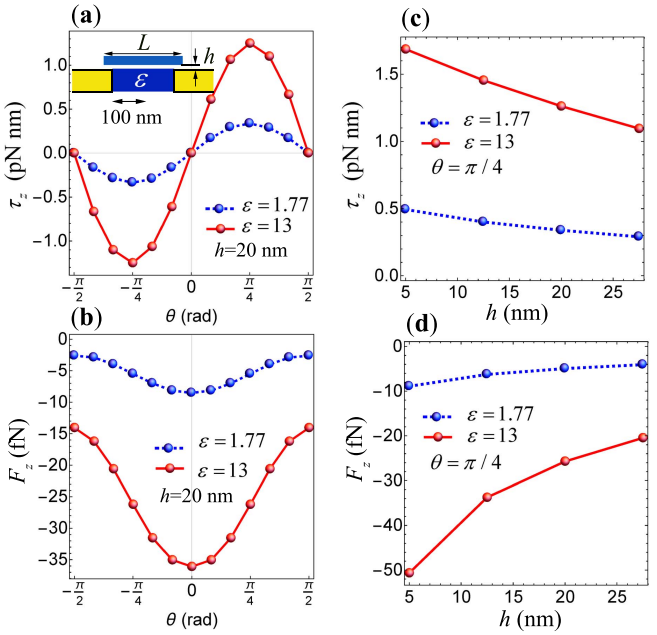

FIG. 3. (color online) (**a-b**) optical torque and (**c-d**) normal optical force on a nanowire ($L = 250\,\text{nm}$, $r = 20\,\text{nm}$) placed on the exit side of a nanohole of radius 100 nm filled with water (dashed lines, $\epsilon = 1.77$) and silicon (solid lines, $\epsilon = 13$) as a function (**a**,**c**) of the angle θ between the nanowire and the incident field polarization direction and (**b**,**d**) of the gap h between the nanowire and the metallic layer. The incident intensity is $I_0 = 1.0\,\text{mW}/\mu\text{m}^2$.

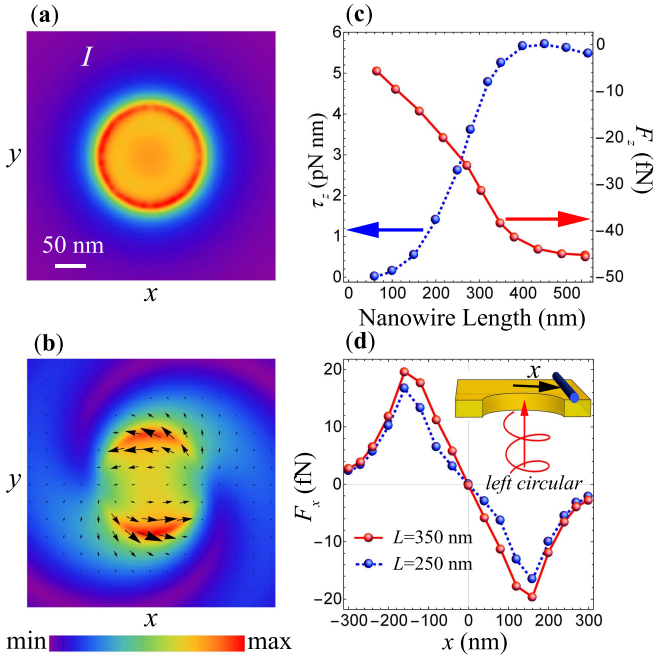

FIG. 4. (**a**) Electric field intensity distribution and (**b**) instantaneous electric field magnitude distribution (shades) and Poynting vector (arrows) in the xy-plane 20 nm above the nanoaperture for left circularly-polarized incident light. (**c**) Optical torque, τ_z, and normal optical force,F_z, for left circularly-polarized incident light as a function of nanowire length L. (**d**) Lateral optical force, F_x, acting on the nanowire for left circularly-polarized incident light for different nanowires with lengths $L = 250$ and 350 nm. In (**c**) and (**d**), $h = 20\,\text{nm}$ and $r = 30nm$. The incident intensity is $I_0 = 1.0\,\text{mW}/\mu\text{m}^{-2}$.

α_{trans} are the polarizabilities along the longitudinal and transverse axis of the ellipsoid [23]. This equation shows that the torque has a sinusoidal behavior with angular period π, which is consistent with the results shown in Fig. 2a. Fig. 2b shows the normal force (F_z), whose negative sign indicates that this is a restoring force pulling the nanowire toward the nanoaperture, where the fields are more enhanced resulting in even stronger transverse and normal trapping forces. Fig. 2c shows the optical torque on nanowires with different lengths. The torque for $\theta = 0$ is negligible in all cases. For $\theta = \pi/2$ the torque increases as the length of the nanowire increases up to a maximum for $L = 350\,\text{nm}$, i.e., when the length of the nanowire is slightly larger than the diameter of the nanohole; a further increase of the nanowire makes its sides go outside the LSP associated to the nanohole and, thus, does not contribute to the overall optical torque. We note that the nanohole confines the nanowire also along the transverse direction, as can be seen in Fig. 2d for the case of the x-direction.

It is also interesting to consider the case when the nanoaperture is filled with a high-index dielectric material. The use of such material, instead of water, in addition to confining the nanowire on a a flat surface, gives the additional advantage of improving the nanoaperture transmission and, thus, of narrowing the transmission resonance [24]. Noting that filling the nanohole shifts the transmission resonance towards a smaller radius/wavelength ratio, we consider a nanoaperture with radius 100 nm in a gold film of thickness 100 nm, i.e., an aperture similar to the one in Fig. 2 but with smaller radius. As shown in Figs. 3a, for such a nanoaperture filled with silicon ($\epsilon = 13$), the optical torque on a nanowire ($L = 250\,\text{nm}$, $r = 20\,\text{nm}$) is enhanced nearly three times compared with the undressed hole. Also the normal optical force is considerably enhanced, as can be seen in Fig. 3b. Both torque (Fig. 3c) and force (Fig. 3d) increase as the gap h between the nanowire and the surface decreases. Therefore, filling nanoapertures with high-index dielectric material can improve the capabilities of the structure and make it more appropriate to efficiently trap and manipulate even smaller particles.

Finally, we will also consider the case of circularly-polarized illumination. In this case, differently from the case of a linearly-polarized incident wave, the average field intensity is ring-shaped near the edge of the nanoaperture, as shown in Fig. 4a. In fact, the two hotspots generated by the instantaneous electric fields (Fig. 4b) rotate around the edge of the nanoaperture at

the frequency of the incident field, leading to a transverse clockwise or counterclockwise energy flow depending on whether the incident wave is left or right circularly-polarized. As can be seen in Figs. 4a and 4b, a plasmonic optical vortex is generated and, thus, the nanoaperture can be thought as a device capable of converting the spin angular momentum (SAM) of the circularly-polarized incident beam to orbital angular momentum (OAM) of the evanescent field. Fig. 4c shows the optical torque (solid line) and normal force (dashed line) acting on a nanowire placed on the exit side of the aperture for left-circularly-polarized illumination. Importantly, although the optical torque and normal force magnitudes are a slightly smaller than the highest corresponding torque and force in the case of linear polarization case (cfr. Fig. 2(c)), they are independent of the nanowire orientation. Fig. 4d shows the lateral optical force on the nanowire for nanowires of length $L = 250$ and 350 nm as a function of their lateral position along the x-direction. The nanowires experience the largest restoring force when moving towards the edges of the nanoaperture, while the central position corresponds to a stable equilibrium.

In conclusion, we have demonstrated that it is possible to use a nanoaperture to trap a nanowire and to control its orientation with very low incident power. Furthermore, we have shown that employing circularly-polarized light it is possible to rotate the nanowire at a constant rotation rate. The simplicity of the nanoaperture geometry will permit easy fabrication of this nanodevice.

GV acknowledges funding from Marie Curie Career Integration Grant (MC-CIG) PCIG11GA-2012-321726. MSA and FK wish to thank the graduate office of the University of Isfahan for their support.

* Corresponding author:mshphy@gmail.com

[1] O. M Maragò, P. H. Jones, P. G. Gucciardi, G. Volpe, and A. C. Ferrari. Optical trapping and manipulation of nanostructures. *Nature Nanotech.*, 8:807–819, 2013.

[2] R. Agarwal, K. Ladavac, Y. Roichman, G. Yu, C. Lieber, and D. Grier. Manipulation and assembly of nanowires with holographic optical traps. *Opt. Express*, 13:8906–8912, 2005.

[3] P. J. Pauzauskie, A. Radenovic, E. Trepagnier, H. Shroff, P. Yang, and J. Liphardt. Optical trapping and integration of semiconductor nanowire assemblies in water. *Nature Materials*, 5:97–101, 2006.

[4] K. Castelino, S. Satyanarayana, and M. Sitti. Manufacturing of two and three-dimensional micro/nanostructures by integrating optical tweezers with chemical assembly. *Robotica*, 23:435–439, 2005.

[5] Y. Nakayama, P. J. Pauzauskie, A. Radenovic, R. M. Onorato, R. J. Saykally, J. Liphardt, and P. Yang. Tunable nanowire nonlinear optical probe. *Nature*, 447:1098–1101, 2007.

[6] A. A. R. Neves, A. Camposeo, S. Pagliara, R. Saija, F. Borghese, P. Denti, M. A. Iatì, R. Cingolani, O. M. Maragò, and D. Pisignano. Rotational dynamics of optically trapped nanofibers. *Opt. Express*, 18:822–830, 2010.

[7] M. Capitanio and F. S. Pavone. Interrogating biology with force: Single molecule high-resolution measurements with optical tweezers. *Biophys. J.*, 105:1293–1303, 2013.

[8] A. Ashkin, J. M. Dziedzic, J. E. Bjorkholm, and S. Chu. Observation of a single-beam gradient force optical trap for dielectric particles. *Opt. Lett.*, 11:288–290, 1986.

[9] P. H. Jones, O. M. Maragó, and G. Volpe. *Optical tweezers: Principles and applications*. Cambridge University Press, 2015.

[10] M. Righini, G. Volpe, C. Girard, D. Petrov, and R. Quidant. Surface plasmon optical tweezers: Tunable optical manipulation in the femtonewton range. *Phys. Rev. Lett.*, 100:186804, 2008.

[11] M. L. Juan, M. Righini, and R. Quidant. Plasmon nano-optical tweezers. *Nature Photon.*, 5:349–356, 2011.

[12] K. Wang, E. Schonbrun, P. Steinvurzel, and K. B. Crozier. Trapping and rotating nanoparticles using a plasmonic nano-tweezer with an integrated heat sink. *Nature Commun.*, 2:469, 2011.

[13] Y. Zhang, J. Wang, J. Shen, Z. Man, W. Shi, C. Min, G. Yuan, S. Zhu, H. P. Urbach, and X. Yuan. Plasmonic hybridization induced trapping and manipulation of a single au nanowire on a metallic surface. *Nano Lett.*, 14:6430–6436, 2014.

[14] F. J. Garcia-Vidal, L. Martin-Moreno, T. W. Ebbesen, and L. Kuipers. Light passing through subwavelength apertures. *Rev. Mod. Phys.*, 82:729, 2010.

[15] C. Genet and T. W. Ebbesen. Light in tiny holes. *Nature*, pages 39–46, 2007.

[16] H. J. Lezec, A. Degiron, E. Devaux, R. A. Linke, L. Martin-Moreno, F. J. Garcia-Vidal, and T. W. Ebbesen. Beaming light from a subwavelength aperture. *Science*, 297:820–822, 2002.

[17] M. L. Juan, R. Gordon, Y. Pang, F. Eftekhari, and R. Quidant. Self-induced back-action optical trapping of dielectric nanoparticles. *Nature Phys.*, 5:915–919, 2009.

[18] T. W. Ebbesen, H. J. Lezec, H. F. Ghaemi, T. Thio, and P. A. Wolff. Extraordinary optical transmission through sub-wavelength hole arrays. *Nature*, 391:667–669, 1998.

[19] A. Degiron, H. J. Lezec, N. Yamamoto, and T. W. Ebbesen. Optical transmission properties of a single subwavelength aperture in a real metal. *Optics Commun.*, 239:61–66, 2004.

[20] A. Taflove and S. C. Hagness. *Computational electrodynamics*. Artech House, 2005.

[21] P. B. Johnson and R.-W. Christy. Optical constants of the noble metals. *Phys. Rev. B*, 6:4370–4379, 1972.

[22] F. Borghese, P. Denti, and R. Saija. *Scattering from model nonspherical particles: Theory and applications to environmental physics*. Springer Verlag, 2007.

[23] M. Washizu, M. Shikida, S.-I. Aizawa, and H. Hotani. Orientation and transformation of flagella in electrostatic field. *IEEE Trans. Ind. Appl.*, 28:1194–1202, 1992.

[24] F. Garcia de Abajo. Light transmission through a single cylindrical hole in a metallic film. *Opt. Express*, 10:1475–1484, 2002.